

See discussions, stats, and author profiles for this publication at: <https://www.researchgate.net/publication/238648305>

Molecular Dynamics Study of the Poly(oxyethylene) Surfactant C 12 E 2 and Water

ARTICLE *in* LANGMUIR · FEBRUARY 2000

Impact Factor: 4.46 · DOI: 10.1021/la9909493

CITATIONS

54

READS

40

4 AUTHORS, INCLUDING:



[Sanjoy Bandyopadhyay](#)

IIT Kharagpur

74 PUBLICATIONS 2,066 CITATIONS

[SEE PROFILE](#)



[Mounir Tarek](#)

University of Lorraine - CNRS

112 PUBLICATIONS 3,068 CITATIONS

[SEE PROFILE](#)

Molecular Dynamics Study of the Poly(oxyethylene) Surfactant $C_{12}E_2$ and Water

Sanjoy Bandyopadhyay,^{*,†} Mounir Tarek,^{†,‡} Matthew L. Lynch,[§] and Michael L. Klein[†]

Center for Molecular Modeling, Department of Chemistry, University of Pennsylvania, Philadelphia, Pennsylvania 19104-6323, NIST Center for Neutron Research, National Institute of Standards and Technology, Gaithersburg, Maryland 20899, and Corporate Research Division, Miami Valley Laboratories, The Procter & Gamble Company, Cincinnati, Ohio 45253-8707

Received July 16, 1999. In Final Form: September 29, 1999

Constant pressure and temperature (*NPT*) molecular dynamics (MD) simulations have been carried out to investigate the properties of a binary mixture of the poly(oxyethylene) surfactant $C_{12}E_2$ and water in its liquid crystalline lamellar phase (L_α). The calculated interlamellar spacing and the area per surfactant were found to be in reasonable agreement with X-ray diffraction results. The water molecules were observed to form hydrogen bonded bridged structures linking the oxygen atoms of the same surfactant chain. This interaction leads to a strong preference for the C–C bonds in the headgroup to attain a gauche conformation.

I. Introduction

The monoalkyl ethers of poly(oxyethylene) glycols, C_mE_n ($C_mH_{2m+1}(OC_2H_4)_nOH$) form an important class of non-ionic surfactants with a wide range of industrial applications, such as detergency, cosmetics, pharmacy, etc.¹ Most of these applications depend on the properties of the surfactants either in solution or at interfaces. These surfactants in aqueous solution exist in different liquid crystalline phases, depending on the length of the alkyl and poly(oxyethylene) chains (m, n), temperature, and surfactant concentration.^{1–6} Tiddy and co-workers² have studied in detail the phase behavior of a series of C_mE_n surfactants using optical microscopy over the temperature range of 0–100 °C. A variety of lyotropic liquid crystalline phases, such as hexagonal, lamellar, and normal and reversed cubic bicontinuous phases, were observed, depending on the temperature and concentration. The structure and morphologies of the intermediate liquid crystalline phases of the $C_{16}E_6$ /water system has been studied in detail by Fairhurst et al.⁴ using X-ray scattering, optical microscopy, and NMR techniques. They observed that, at intermediate concentration and temperature, an aqueous solution of $C_{16}E_6$ exhibits interesting phase behavior, the high-temperature lamellar phase and the low-temperature two-phase region of hexagonal and gel phases. A wide range of intermediate phases of the $C_{16}E_6$ /water system were also reported by Funari et al.⁵ It was

recently observed that $C_{12}E_n$ compounds with a short oxyethylene chain (e.g., $C_{12}E_2$, $C_{12}E_3$) exhibit a rich variety of intermediate liquid crystalline phases within a narrow range of temperature and concentration.^{6,7} Funari and Rapp⁶ used time-resolved X-ray diffraction to study different phases of a binary mixture of $C_{12}E_2$ and water. They observed transformations from lamellar to two different cubic phases, while heating at an intermediate concentration range. Recently, Lynch et al.⁷ reported the aqueous phase behavior of $C_{12}E_2$ using diffusive interfacial transport–near-infrared method (DIT-NIR), a new technique for obtaining accurate phase diagrams. They showed the existence of different liquid crystalline phases, including a lamellar phase, a sponge phase, and two bicontinuous cubic phases within a narrow temperature and composition range and provide a significant improvement to the currently accepted phase diagrams of $C_{12}E_2$.

Proper knowledge of the headgroup conformation and their solvation is essential for obtaining a molecular level understanding of the complicated phase behavior of such systems. Theoretical calculations and computer simulation studies can play a major role toward this objective. Andersson and Karlström⁸ carried out quantum chemical calculations on the conformational structure of 1,2-dimethyloxyethane, both in the gas phase and in different polar solvents. They showed that their model favors the C–C bond to be in the gauche form rather than trans, in agreement with NMR studies on similar systems.^{9,10} These calculations were extended to explain the critical solution phenomena in poly(ethylene oxide) (PEO) solutions,¹¹ and dynamics and order in micellar solutions of $C_{12}E_n$ and the surfactant neat liquids.¹² There are few simulation studies attempted on these systems with explicit atomistic models. Kong et al.^{13,14} have reported Monte Carlo simulations of single $C_{12}E_2$ and $C_{12}E_3$ surfactant chain headgroups

* To whom correspondence should be addressed. Telephone: (215) 573-4773. Fax: (215) 573-6233. E-mail: sanjoy@cmm.chem.upenn.edu.

[†] University of Pennsylvania.

[‡] National Institute of Standards and Technology.

[§] The Procter & Gamble Co.

(1) Laughlin, R. G. *The Aqueous Phase Behavior of Surfactants*; Academic Press: New York, 1994.

(2) Mitchell, D. J.; Tiddy, G. J. T.; Waring, L.; Bostock, T.; McDonald, M. P. *J. Chem. Soc., Faraday Trans. 1* **1983**, 79, 975–1000.

(3) Roux, D.; Coulon, C.; Cates, M. E. *J. Phys. Chem.* **1992**, 96, 4174–4187.

(4) Fairhurst, C. E.; Holmes, M. C.; Leaver, M. S. *Langmuir* **1997**, 13, 4964–4975.

(5) Funari, S. S.; Holmes, M. C.; Tiddy, G. J. T. *J. Phys. Chem.* **1994**, 98, 3015–3023.

(6) Funari, S. S.; Rapp, G. *J. Phys. Chem. B* **1997**, 101, 732–739.

(7) Lynch, M. L.; Kochvar, K. A.; Burns, J. L.; Laughlin, R. G. *J. Phys. Chem.*, submitted for publication.

(8) Andersson, M.; Karlström, G. *J. Phys. Chem.* **1985**, 89, 4957–4962.

(9) Viti, V.; Zampetti, P. *Chem. Phys.* **1973**, 2, 233–238.

(10) Viti, V.; Indovina, P. L.; Podo, F.; Radics, L.; Nemety, G. *Mol. Phys.* **1974**, 27, 541–559.

(11) Karlström, G. *J. Phys. Chem.* **1985**, 89, 4962–4964.

(12) Ahlén, T.; Karlström, G.; Lindman, B. *J. Phys. Chem.* **1987**, 91, 4030–4036.

attached to the hydrophobic wall of a bilayer. They studied the conformation of the headgroup and the structure of water around it. Atomic based molecular dynamics (MD) simulations can play a crucial role in elucidating the structural and conformational properties of these systems at a microscopic level and are therefore considered as a natural complement to experiments. Recently, Tasaki¹⁵ reported conformational properties of a PEO chain in aqueous solution using MD techniques. In this article, we present MD simulation results of a binary mixture of $C_{12}E_2$ and water in liquid crystalline lamellar phase (L_α), with eight water molecules per surfactant chain, at a temperature of 23 °C. In the next section we discuss the potential model, system setup, and the simulation details. Then the results are presented and compared with experimental data and theoretical calculations.

II. System Setup and Simulation Details

The initial configuration of our constant pressure (*NPT*) simulation system was set up by arranging a monolayer of 32 $C_{12}E_2$ molecules on a 4×4 body-centered square lattice in the *xy* plane with hydrocarbon chains in all trans conformations extending perpendicular to the lattice plane. The initial lattice constants were chosen to give the surface area/molecule of 34 \AA^2 , corresponding to the value for adsorption at the air/water interface at the critical micelle concentration (cmc).¹⁶ Two such Langmuir type monolayers were placed, with their headgroups solvated, in the *xy* plane of a roughly 14 \AA thick slab of 512 water molecules (8 water per headgroup). Such an initial arrangement led to a box dimension of approximately 64 \AA along the *z* direction (perpendicular to the bilayer plane, *xy*). The concentration of the system corresponded to 65.6 wt % of the surfactant.

A short MD run of 2 ps was first performed at 1000 K, keeping the surfactant headgroups and the water molecules fixed, to randomize the hydrocarbon chain conformations. The resulting configuration was then equilibrated at constant temperature ($T = 23 \text{ °C}$) and pressure ($P = 0$) for 1 ns. This equilibration period was followed by an *NPT* production run of 2 ns duration with isotropic cell fluctuations. The *NPT* runs utilized the Nosé–Hoover chain thermostat extended system method¹⁷ as implemented in the PINY-MD computational package.¹⁸ A recently developed reversible multiple time step algorithm¹⁷ allowed us to employ a 4 fs MD time step. This was achieved using a three-stage force decomposition into intramolecular forces (torsion/bond bend), short-range intermolecular forces (a 7.0 \AA RESPA cutoff distance), and long-range intermolecular forces. Electrostatic interactions were calculated by using the particle-mesh Ewald (PME) method.¹⁹ The minimum image convention²⁰ was employed to calculate the Lennard-Jones interactions and the real-space part of the Ewald sum using a spherical truncation of 7.0 and 10 \AA , respectively, for the short- and the long-range parts of the RESPA decomposition. “SHAKE/ROLL” and “RATTLE/ROLL” methods¹⁷ were implemented to constrain all bonds involving H atoms to their equilibrium values.

The intermolecular potential model was based on pairwise additive site–site electrostatic and Lennard-Jones contributions. The rigid three-site SPC/E model²¹ was employed for water. The CH_3 and CH_2 groups of the surfactants were treated as united

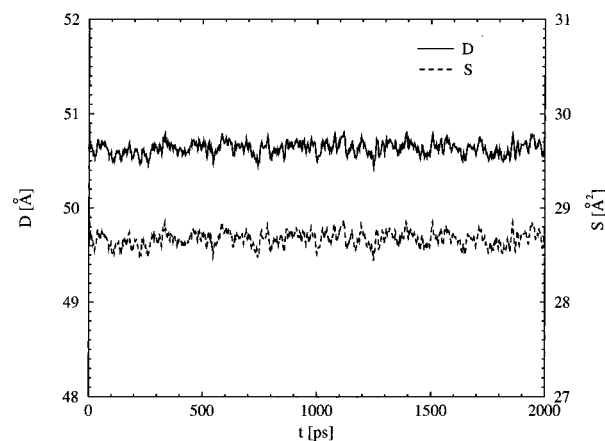


Figure 1. Time evolution of the interlamellar spacing D (solid line) and the area per molecule S (dashed line) during the last 2 ns of the simulation of the lamellar phase (L_α) of $C_{12}E_2$ at 23 °C.

Table 1. Comparison of MD and Experimental Values of the Interlamellar Spacing (D) and Area per Molecule (S) in the Lamellar Phase (L_α) of the $C_{12}E_2$ /Water System

quantity	MD	expt ^a
D (Å)	50.6 ± 0.06	48.2
S (Å ²)	28.7 ± 0.07	30

^a Interpolated data obtained from ref 6.

atoms (i.e. these groups were represented by single interaction sites). The potential parameters for the alkane chain groups were taken from the work of Martin and Siepmann,²² while the EO groups were modeled using the OPLS parameters.^{23,24} The surfactant chains were made flexible by including bond stretching, bending, and torsion interactions.

III. Results and Discussion

The time evolution of the interlamellar spacing (D) and the surface area per molecule (S) over the last 2 ns of the simulation run are shown in Figure 1. These quantities fluctuated but did not show any drift during the 2 ns production run. This indicates that the bilayer structure was equilibrated during the previous 1 ns run. The average values calculated from the simulation are compared in Table 1 with X-ray diffraction studies of Funari and Rapp⁶ under similar conditions. The calculated values of these structural quantities are in reasonable agreement with experimental measurements. To verify whether these calculated quantities depend on the choice of water model, we carried out another MD run of 500 ps duration, using the TIP3P model²⁵ for water. We observed that the values of interlamellar spacing (D) and area per molecule (S) were independent of the model employed for water.

Figure 2 shows snapshots (cross-sectional view perpendicular to the bilayer plane) of the configuration of the system near the beginning (a) and at the end (b) of the simulation run. The important feature to note from Figure 2 is the structure of the headgroup regions at the bilayer interface. It is clear that in the course of the simulation significant roughness developed near the surfactant headgroup region of the interface as compared to the nearly flat interface at the beginning of the run. The number

(13) Kong, Y. C.; Nicholson, D.; Parsonage, N. G.; Thompson, L. J. *Chem. Soc., Faraday Trans.* **1994**, *90*, 2375–2380.

(14) Kong, Y. C.; Nicholson, D.; Parsonage, N. G.; Thompson, L. J. *Chem. Soc., Faraday Trans.* **1995**, *91*, 4261–4268.

(15) Tasaki, K. *J. Am. Chem. Soc.* **1996**, *118*, 8459–8469.

(16) Lu, J. R.; Li, Z. X.; Su, T. J.; Thomas, R. K.; Penfold, J. *Langmuir* **1993**, *9*, 2408–2416.

(17) Martyna, G. J.; Tuckerman, M. E.; Tobias, D. J.; Klein, M. L. *Mol. Phys.* **1996**, *87*, 1117–1157.

(18) Martyna, G. J.; Samuelson, S.; Hughs, A.; Tobias, D. J.; Yarne, D.; Klein, M. L.; Tuckerman, M. E. Preprint.

(19) Darden, T.; York, D.; Pedersen, L. *J. Chem. Phys.* **1993**, *98*, 10089.

(20) Allen, M. P.; Tildesley, D. J. *Computer Simulation of Liquids*; Clarendon: Oxford, U.K., 1987.

(21) Berendsen, H. J. C.; Grigera, J. R.; Straatsma, T. P. *J. Phys. Chem.* **1987**, *91*, 6269.

(22) Martin, M. G.; Siepmann, J. I. *J. Phys. Chem. B* **1998**, *102*, 2569–2577.

(23) Jorgensen, W. L. *J. Phys. Chem.* **1986**, *90*, 1276–1284.

(24) Briggs, J. M.; Matsui, T.; Jorgensen, W. L. *J. Comput. Chem.* **1990**, *11*, 958–971.

(25) Jorgensen, W. L.; Chandrasekhar, J.; Madura, J. D.; Impey, R. W.; Klein, M. L. *J. Chem. Phys.* **1983**, *79*, 926–935.

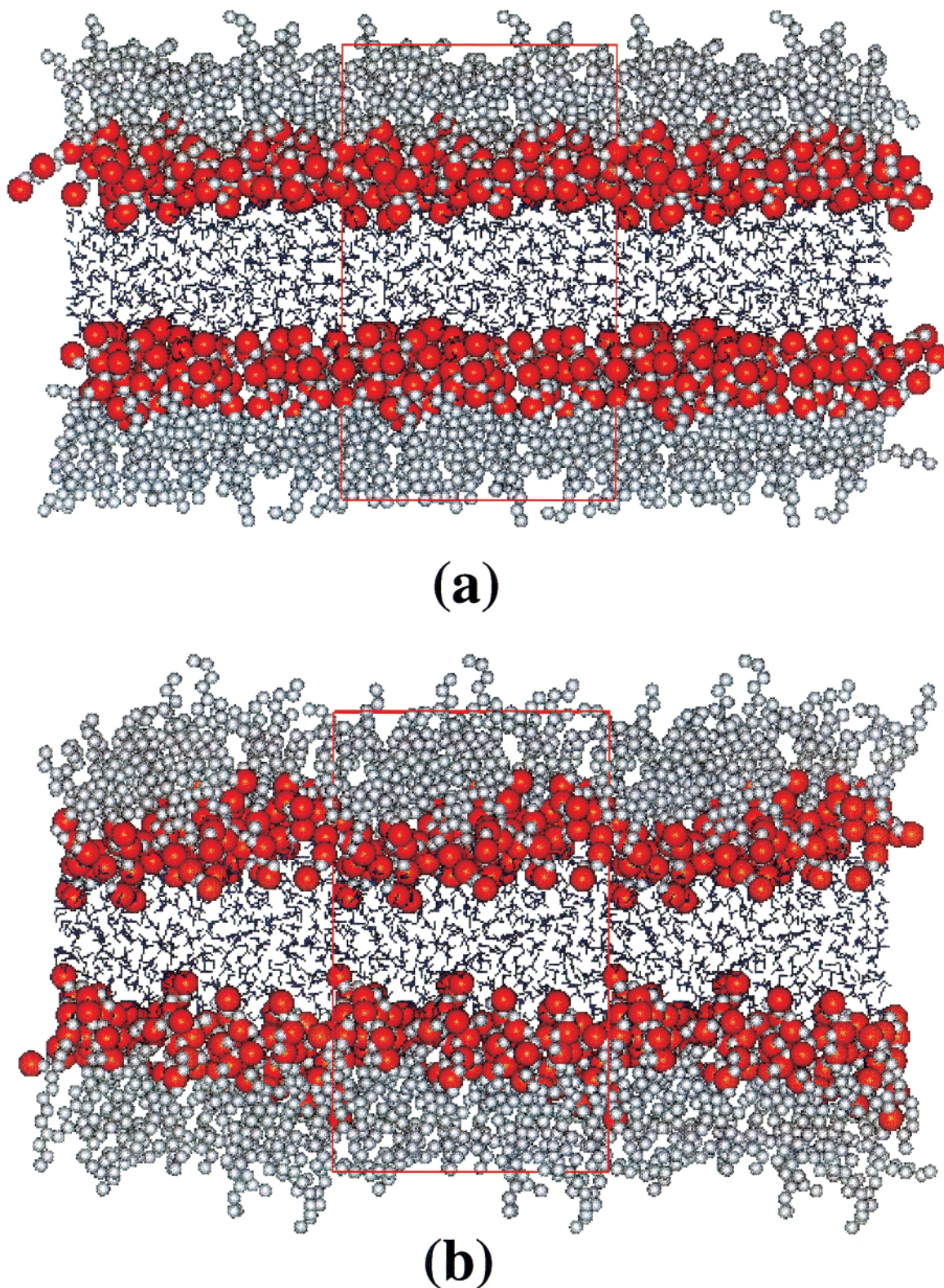


Figure 2. Snapshots of the configuration of the system near the beginning (a) and at the end (b) of the simulation. The headgroup oxygen atoms are drawn as van der Waals spheres (red), while the CH_3 and CH_2 groups are drawn according to their covalent radii (grey), and the water molecules are drawn as sticks. The system is replicated once on both sides of the central simulation cell for visual clarity.

density profiles of the terminal hydroxyl groups (OH), oxyethylene groups (EO), hydrocarbon chain atoms, and the water molecules, from the bilayer center and normal to the plane of the bilayer, are shown in Figure 3. The main features of this plot are similar to the well-known picture of the surfactant organization at an interface.^{26–30}

The headgroups are all located at the interface and are hydrated. Only a small amount of water penetrated within

(26) Tarek, M.; Tobias, D. J.; Klein, M. L. *J. Phys. Chem.* **1995**, *99*, 1393–1402.

(27) Tu, K.; Tobias, D. J.; Blasie, J. K.; Klein, M. L. *Biophys. J.* **1996**, *70*, 595–608.

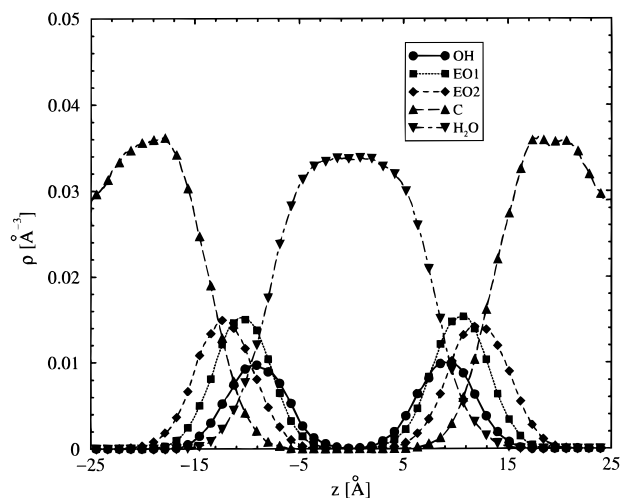


Figure 3. Number density profiles of the hydroxyl groups (OH), oxyethylene groups (EO), hydrocarbon chain atoms, and water molecules, measured with respect to the center of the bilayer in the direction (z) normal to the bilayer plane.

the hydrocarbon tail part of the bilayer, and there is a large fraction of dry region within the hydrocarbon chains of the surfactants.

The conformation of the headgroups and the structure of water molecules around them are crucial issues in determining the surfactant behavior in liquid crystalline phases. We calculated the relative conformational population of the torsional angles around the C–C and C–O bonds in the headgroup region of the surfactant. A strong preference was observed for the C–C bonds to remain in gauche form, while the two adjacent C–O bonds were found to favor a trans conformation. Specifically, 97% of the C–C bonds were gauche, while approximately 80% of the C–O bonds were trans. It was observed that the water molecules have strong tendencies to form H-bonds bridging between the two adjacent ethylene glycol oxygen atoms of the same surfactant chain. A representative configuration of a surfactant chain with a water molecule forming a bridged H-bonded structure is shown in Figure 4. Such a bridging structure is favored if the C3–C4 bond attains gauche conformation and the adjacent C3–O2 and C4–O3 bonds remain in trans form (see Figure 4). Therefore, the main reason for overwhelmingly large fraction of gauche C3–C4 bonds in the surfactant headgroup region is likely the tendency to form such H-bonded bridged structures with water. Similar behavior was observed when a single $C_{12}E_2$ chain was fixed on a hydrocarbon wall in water.¹³ Also, recently, Heymann and Grubmüller³¹ have shown that solvent water forms similar H-bonded bridged structures with poly(ethylene glycol) polymers (PEG), which in turn has a strong influence on the elastic properties of the hydrated polymer. Similar H-bonded bridged structures were also observed in a MD study of PEO in aqueous solution.¹⁵

To obtain more insight into the structure of water close to the surfactants, radial distribution functions, $g(r)$, of different atoms in the headgroup region with water were calculated and are displayed in Figure 5. A strong first

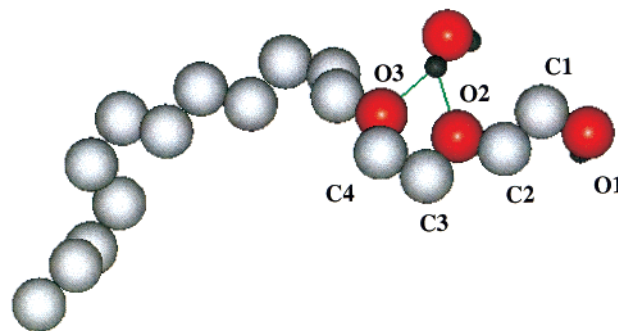


Figure 4. Representative snapshot of a water molecule forming a bridged H-bonded structure with the ethylene glycol oxygen atoms of a surfactant chain. The hydrocarbon chain atoms, oxygens, and the hydrogen atoms are drawn as gray, red, and dark green spheres, while the H-bonds are shown as green lines. Note that the headgroup atoms of the chain are labeled for clarity.

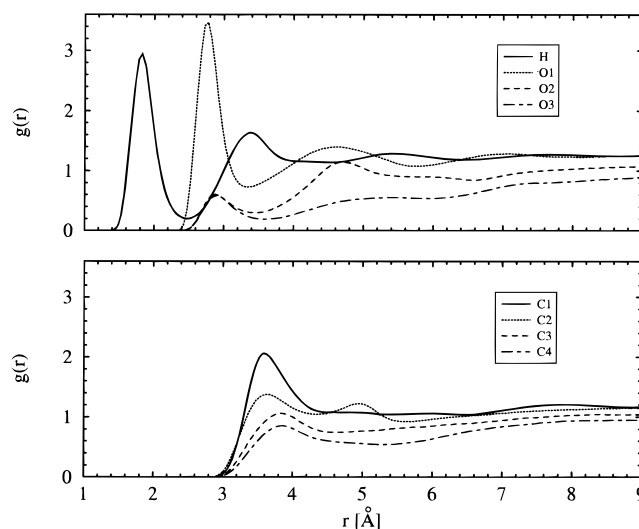


Figure 5. Radial distribution functions of the headgroup atoms of $C_{12}E_2$ surfactant with water oxygen atoms. The surfactant atoms are labeled as shown in Figure 4.

peak around 2.8 Å, corresponding to the nearest neighbor distance between oxygen atoms, is observed for the hydroxyl group oxygen atoms (O1). The intensity of this peak decreases for the oxygen atoms of the oxyethylene groups (O2 and O3), as they become further apart from the aqueous layer. There is a broad peak with sufficient intensity for the O2 atoms, which corresponds to the water molecules hydrogen bonded to O1. We calculated the number of water molecules that are nearest neighbors to the oxygen atoms of the surfactants, by integrating up to ~ 3.5 Å of the corresponding radial distribution function. It was found that, on average, there are approximately 2 water molecules per oxygen atom of the hydroxyl group (O1) and 0.5 per oxygen atom of the oxyethylene groups (O2, O3). The strong peak around 2 Å for the water oxygen atoms and the H atoms of the surfactant hydroxyl group also shows the presence of hydrogen-bonded water molecules. The water distributions around headgroup carbon atoms are generally of low intensity. However, there is some evidence of structured water molecules around the first carbon atom, C1, with a nearest neighbor maximum around 3.6 Å. To gain further insight into the spatial three-dimensional distribution of water molecules around the oxygen atoms of the surfactant headgroups, we calculated the local density isosurfaces of the water molecules around

(28) Bandyopadhyay, S.; Klein, M. L.; Martyna, G. J.; Tarek, M. *Mol. Phys.* **1998**, *95*, 377–384.

(29) Schweighofer, K. J.; Essmann, U.; Berkowitz, M. *J. Phys. Chem. B* **1997**, *101*, 10775–10780.

(30) Forester, T. R.; Smith, W.; Clarke, J. H. R. *J. Chem. Soc., Faraday Trans.* **1997**, *93*, 613–619.

(31) Heymann, B.; Grubmüller, H. *Chem. Phys. Lett.* **1999**, *307*, 425–432.

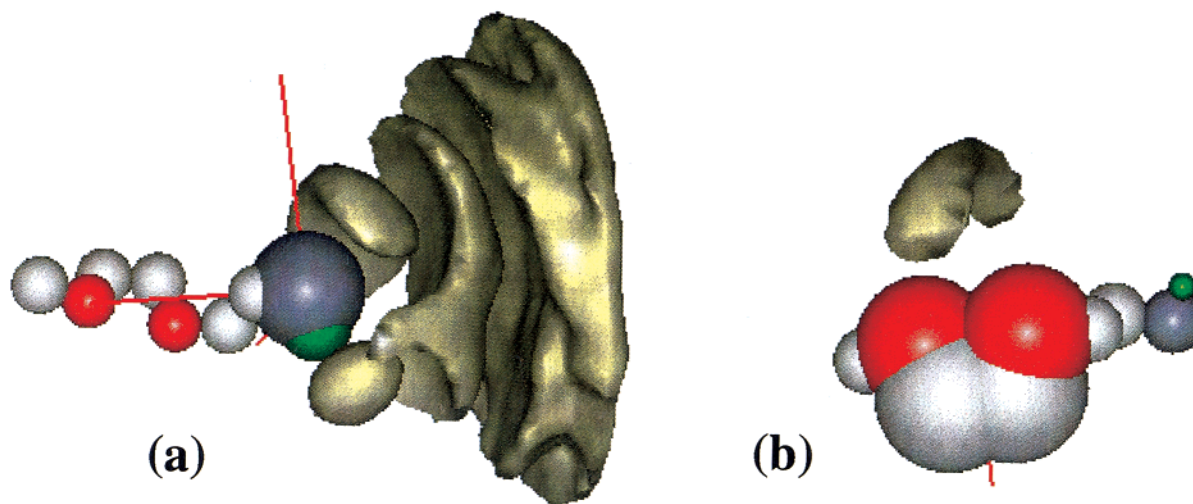


Figure 6. Ensemble average density isosurfaces of the water oxygen atoms around (a) a representative terminal hydroxyl group of the surfactant and (b) a representative oxyethylene group, O2–C3–C4–O3. The entire oxyethylene part of the surfactant chain is drawn for clarity. The representative atoms in each case are drawn according to their van der Waals radii, while the other atoms are drawn with their covalent radii. The atom coloring scheme is as follows: H, green; hydroxyl group O, blue; oxyethylene group O, red; C, gray.

the hydroxyl group oxygen atoms (O1) and the O2–C3–C4–O3 groups. These distributions are illustrated in Figure 6. To generate the isosurfaces, first, the instantaneous positions of the atoms in question were replaced by normalized Gaussian distributions with a width of 0.4 Å, to obtain a smooth effective local density.^{26,32} A surface of the nuclear distribution was then obtained by linear interpolation of the contours generated over last 2 ns of the production run. Density surfaces corresponding to the water molecules hydrogen bonded to the terminal OH group, as well as those for a few higher level neighboring shells, are displayed in Figure 6a. These densities reveal that the water around the terminal OH group is highly structured, in accordance with the corresponding $g(r)$ plot (see Figure 5). Figure 6b shows the density distribution of the water molecules bridging between the oxyethylene group oxygen atoms (O2, O3), which favor the formation of C3–C4 gauche bonds.

IV. Conclusion

In this paper we presented results of a MD simulation of the lamellar phase (L_α) of the nonionic surfactant $C_{12}E_2$. The structural properties of the system, such as the interlamellar spacing (D) and the area per surfactant (S), were found to be in reasonable agreement with X-ray diffraction data. The conformational properties and the distribution of water molecules around the surfactant headgroups were investigated in detail. We observed that there is a tendency for water molecules to form hydrogen-bonded bridged structures between the oxygen atoms of a surfactant chain. This leads to headgroup conformations where the C–C bonds tend to remain in gauche form, while the adjacent C–O bonds tend to remain in trans conformation.

Acknowledgment. This work was supported by generous grants from the Procter & Gamble Co. and the National Science Foundation. We thank John Shelley and Bill Laidig for insightful comments on our simulations.

(32) Shelley, J. C.; Sprik, M.; Klein, M. L. *Langmuir* **1993**, 9, 916–926.